# Austral winter external and internal atmospheric variability between 1980 and 2014

Hui Ding[1], Richard J. Greatbatch[1,2], Hai Lin[3], Felicitas Hansen[1], Gereon Gollan[1], and Thomas Jung[4]

[1]GEOMAR Helmholtz Centre for Ocean Research Kiel, Kiel, Germany, [2]Faculty of Mathematics and Natural Sciences, University of Kiel, Kiel, Germany, [3]MRD/ASTD, Environment and Climate Change Canada, Dorval, Quebec, Canada, [4]Alfred-Wegener-Institut für Polar-und Meeresforschung, Bremerhaven, Germany

**Abstract** We examine the interannual variability of the seasonal mean atmospheric circulation in the Southern Hemisphere during austral winter. The three major modes are identified by rotated empirical orthogonal function (REOF) analysis. As expected, REOF1 is associated with the Southern Annular Mode which is dominated by internal atmospheric dynamics. REOF2 displays a wave train, linked to the western North Pacific monsoon and the Pacific-Japan pattern in East Asia in the same season; REOF3 resembles the Pacific-South American pattern. Externally forced variability strongly projects on both REOF2 and REOF3 so that in the ensemble mean, an atmospheric model with prescribed observed sea surface temperature captures considerable parts of the time evolution of REOF2 (50%) and REOF3 (25%), suggesting a potential predictability for the two modes.

## 1. Introduction

In the extratropical Southern Hemisphere (SH), the variability of the atmospheric circulation is dominated by the Southern Annular Mode (SAM) throughout the year [*Thompson and Wallace*, 2000; *Baldwin*, 2001]. The SAM is characterized by a roughly zonally symmetric dipole structure with opposing centers of action near 40° and 65°S in the meridional direction and an equivalent barotropic structure in the vertical. The existence of the SAM is generally attributed to internal atmospheric dynamics, limiting its predictability.

The impact of tropical sea surface temperature (SST) on the austral summer (December/January/February; DJF) SH extratropical atmospheric circulation has been extensively studied. Many observational and modeling studies have shown that El Niño–Southern Oscillation (ENSO) exerts a significant impact on the SAM during austral summer when ENSO matures and peaks [e.g., *Zhou and Yu*, 2004; *Grassi et al.*, 2005; *L'Heureux and Thompson*, 2006; *Fogt and Bromwich*, 2006; *Ding et al.*, 2012; *Ding and Steig*, 2013; *Ding et al.*, 2015], though this influence is modulated decadally by other factors [*Ding et al.*, 2015].

By contrast, the interannual variability of the SH extratropical atmospheric circulation during the austral winter season (June/July/August; JJA) has received comparatively little attention. The observed signature of ENSO on the SH extratropical zonal mean circulation is weak and not significant in austral winter because of relatively weak SST variations in the tropics in this season [*L'Heureux and Thompson*, 2006]. However, SH extratropical atmospheric circulation variations display a significant zonal asymmetry in this season [*Ding et al.*, 2012]. Based on observational data, *Ding et al.* [2012] showed that in the Pacific sector, SST anomalies in the central tropical Pacific exert an appreciable impact on the SH climate via the Pacific South American pattern [*Karoly*, 1989] whereas in the Indian Ocean sector, eddy/mean flow interaction dominates the dynamics. Thus, both external and internal variability can significantly affect the SH climate in austral winter.

*Lin* [2009] found that convective activity associated with the western North Pacific summer monsoon induces a wave train that affects the extratropical SH climate. The western North Pacific summer monsoon displays a high reproducibility and thus predictability since the 1970s [*Li et al.*, 2012, 2014, 2015]. This implies that the time evolution associated with the SH wave train identified by *Lin* [2009] is also likely reproducible in an numerical model to some extent.

In this study, we examine externally forced and internal components of interannual variability of the austral winter SH atmospheric circulation. Externally forced variations are separated from internal variations based on an ensemble of atmospheric model integrations forced by observed historical SST data. Furthermore,

the SST-induced reproducibility of the external components is further investigated, which defines an upper limit on predictability. In section 2, the models and the experimental procedures are described. Section 3 presents the results, and section 4 provides a summary and discussion.

## 2. Experiments and Methodology

We employ a version of the European Centre for Medium-Range Weather Forecasts (ECMWF) atmosphere model, which was run at a horizontal resolution of T255 with 60 levels in the vertical, the same as used to create the ERA-Interim reanalysis data [*Dee et al.*, 2011]. An ensemble of experiments is performed. In the experiments, the model sees the time series of observed global SST and sea ice [*Dee et al.*, 2011] at the lower boundary. Hereafter, this experiment is denoted as OBS-NO. For each austral winter from 1980 to 2014, an ensemble of nine members was integrated. Each of the nine members was run with a slightly different initial condition taken from around the beginning of May and run forward to the end of August.

The ensemble mean is performed to dampen internal variability and defined as the externally forced variability while internal variability is defined as the deviations from the ensemble mean. This method has been employed in many previous studies [e.g., *Rowell et al.*, 1995; *Lu et al.*, 2006]. The underlying assumption is that internal variability has the same statistical properties in each year and that the effect of perturbing initial conditions has only a random effect on simulated seasonal variations among ensemble members [e.g., *Rowell et al.*, 1995; *Lu et al.*, 2006].

## 3. Results

A varimax rotated empirical orthogonal function [*von Storch and Zwiers*, 2002] analysis was performed on the austral winter (JJA) seasonal mean 500 hPa height (Z500) anomalies to investigate the dominant features of atmospheric circulation over the extratropical Southern Hemisphere (domain 30°S poleward). Hereafter, the spatial pattern of rotated empirical orthogonal function (EOF) is denoted as REOF while the corresponding time evolution is denoted as the rotated principal component (RPC). Z500 is from the ERA-Interim reanalysis [*Dee et al.*, 2011]. Prior to the analysis, the seasonal mean climatology has been removed to calculate anomalies, which are then weighted by the square root of cosine of latitude to provide equal weighting of equal areas. To emphasize interannual variability, all time series are detrended. The varimax rotation technique removes the orthogonality constraint on EOFs, leading to more localized and at the same time more physically meaningful spatial patterns [*von Storch and Zwiers*, 2002]. According to *North et al.* [1982], only the first three REOFs (Figures 1 and 2) calculated from ERA-Interim can be significantly separated from each other and from the remaining REOFs, so that they are the subject of focus in this study. In addition, we have repeated the analyses using Z200 and Z700 from ERA-Interim (Figures S1 and S2 in the supporting information) [*Dee et al.*, 2011] and Z200/Z500/Z700 from National Centers for Environmental Prediction (not shown) [*Kalnay et al.*, 1996], and the corresponding spatial patterns of the leading REOFs show no qualitative change.

REOF-1 of ERA-Interim is shown in Figure 1a. It explains 27.8% of the variance and displays the well-known features associated with the SAM. It is expected that the SAM, the dominant mode, is captured by the first EOF [e.g., *Thompson and Wallace*, 2000; *Ding et al.*, 2012]. The correlation (not shown) between the first principal component and tropical SST is weak and not significant at the 95% level, consistent with the finding that the ENSO projection onto the SAM is weak during austral winter [*L'Heureux and Thompson*, 2006]. Compared to the spatial pattern of EOF-1 without rotation (Figure S3), the varimax rotation reduces the loading of action in the Pacific sector near 110°W but maintains the pattern in the Indian Ocean sector (Figure 1a). *Ding et al.* [2012] also note that internal atmospheric dynamics (i.e., eddy/mean flow interaction) play a more important role in the Indian Ocean sector than the Pacific sector.

REOF-2 from the ensemble mean of OBS-NO (Figure 1b), explaining 20.6% of the variance, displays the basic spatial features associated with the SAM (Figure 1a) although the SAM is mainly an atmospheric internal mode, and the ensemble mean is mainly composed of an SST-forced external component. This is probably because performing ensemble mean over nine ensemble members does not suffice to dampen all internal variability. Nevertheless, the correlation between RPC-1 of ERA-Interim and RPC-2 of the ensemble mean of OBS-NO is only −0.1 (Figure 1c), further confirming that the SST-forced external component has only a negligible effect on the time evolution of the austral winter SAM which is primarily dominated by internal atmospheric dynamics. The rotated EOF analysis has also been performed on the internal components of OBS-NO.
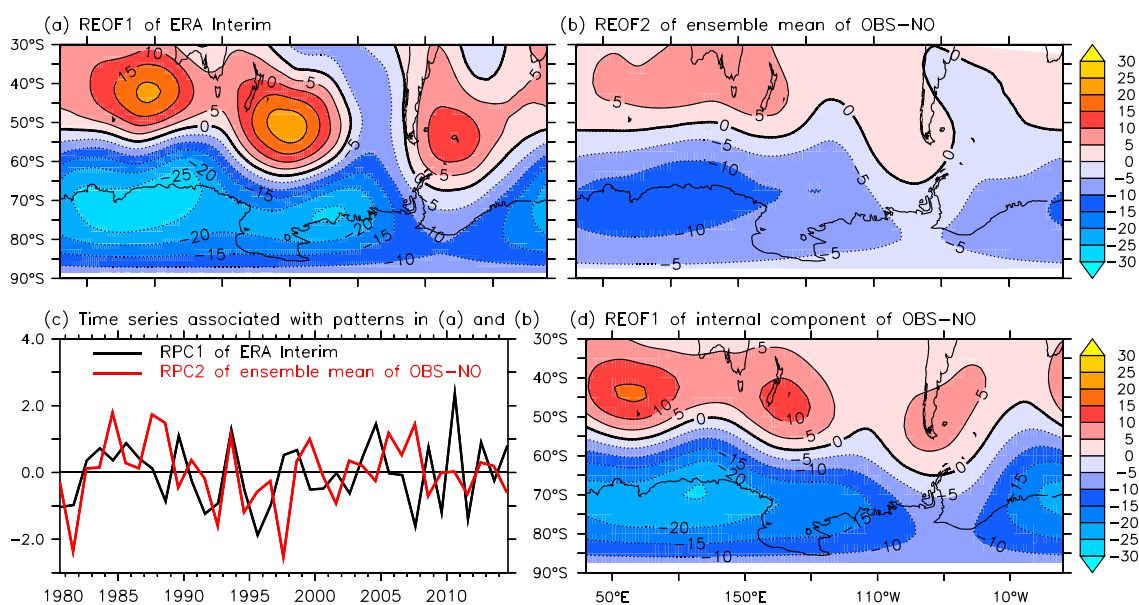
**Figure 1.** Spatial patterns of (a) REOF-1 of ERA-Interim (explaining 27.8% of the variance), (b) REOF-2 of the ensemble mean of OBS-NO (explaining 20.6% of the variance), and their principal components are shown in Figure 1c. (c) The RPCs are normalized by their own standard deviation which is now carried by the corresponding spatial pattern shown in Figures 1a and 1b. (d) The spatial patterns of REOF-1 (explaining 23.3% of the variance) calculated from the internal component of OBS-NO, also carrying the standard deviation of the corresponding RPC (not shown).

Not surprisingly, the SAM comes out as the first REOF mode and explains 23.3% of the variance in the internal variability (Figure 1d).

REOF-2 of ERA-Interim, which explains 17.7% of the variance, is characterized by a wave train emanating from the south of Australia (Figure 2a). We note that its spatial pattern (Figure 2a) closely resembles the teleconnection pattern associated with the western North Pacific monsoon (WNPM) identified by *Lin* [2009]. Following *Wang and Fan* [1999] and *Li et al.* [2014], the WF (Wang and Fan) index (Figure 2d) is defined as the difference of the boreal summer (austral winter) mean 850 hPa zonal wind anomalies between (90°–130°E, 5°–15°N) and (110°–140°E, 20°–30°N). The WF index measures the interannual variability of the western North Pacific monsoon [*Li et al.*, 2014]. The correlation between the WF index and the principal component associated with REOF-2 (RPC-2) is −0.4 (significantly different from zero at the 95% confidence level). *Sun et al.* [2010] also pointed out that the WF index is highly correlated (see Figure 2d) with the leading mode of interannual fluctuations of the East Asian Summer (JJA; austral winter) Monsoon (EASM), also known as the Pacific-Japan (P-J) pattern [*Nitta*, 1987]. Following *Sun et al.* [2010], and also see the supporting information (Figure S4), the time evolution of the leading mode of the EASM is calculated and denoted as the P-J index hereafter. From Figure 2d, it is apparent that there is a significant link between the EASM and REOF-2 of ERA-Interim; the correlation is −0.35 (significant at the 95% level) between the P-J index and RPC-2 of ERA-Interim.

We now turn to the reproducibility of the time evolution associated with REOF-2. Given that the western North Pacific climate is dominated by the externally forced component [*Lu et al.*, 2006], that the WNPM displays a high predictability [*Li et al.*, 2012, 2014, 2015] and the link between the WNPM and REOF-2 of ERA-Interim, we speculate that the externally forced component at least partly projects onto the spatial pattern associated with REOF-2 (Figure 2a) so that its time evolution is at least partly reproducible. Indeed, the ensemble mean of OBS-NO captures the major spatial features noted in REOF-2 of ERA-Interim (Figure 2a) in its REOF-3 (Figure 2c), explaining 10.2% of the variance, despite smaller amplitude. The smaller amplitude is likely because performing the ensemble mean dampens internal variability in the model whereas there is the likelihood that in ERA-Interim, some internal variability projects on to this mode. It is also possible that the model underestimates the magnitude of the mode due to model error. In any case, the corresponding principal components of the two REOFs (Figures 2a and 2b) are shown in Figure 2c, and the correlation between them is around 0.7 (significantly different from zero at the 95% confidence level) from 1980 to 2014. It follows that the ensemble mean captures about 50% of variability associated with the second mode in ERA-Interim, confirming that externally forced variability strongly projects onto this mode.
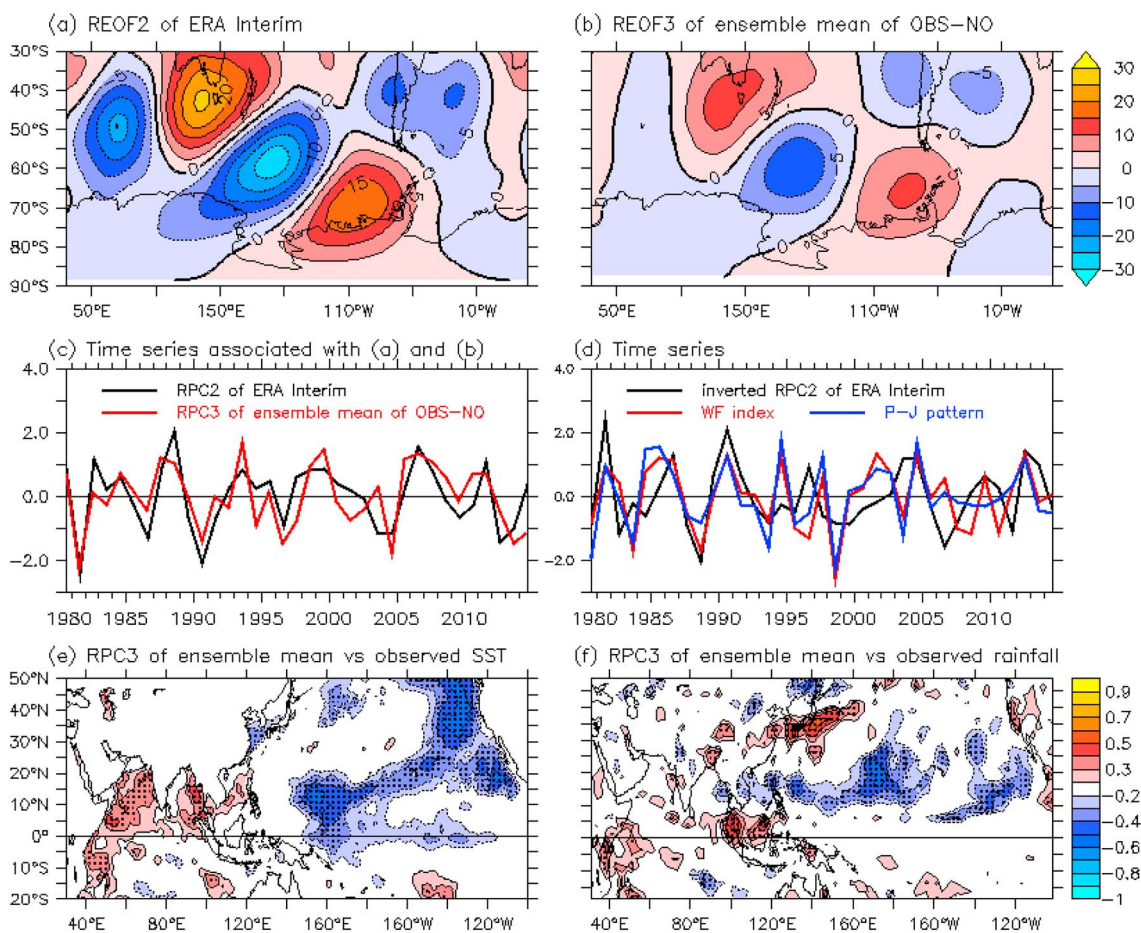
**Figure 2.** Spatial patterns of (a) REOF-2 of ERA-Interim (explaining 17.7% of the variance), (b) REOF-3 of the ensemble mean of OBS-NO (explaining 10.2% of the variance), and their principal components (RPC) are shown in Figure 2c. (c) The RPCs are normalized by their own standard deviation which is now carried by the corresponding spatial pattern shown in Figures 2a and 2b. (d) The inverse of RPC-2 of ERA-Interim, the WF index, and the P-J index (see the body text for the definitions of the WF index and the P-J index, both of which are calculated using ERA-Interim). (e and f) The correlation between RPC-3 of the ensemble mean of OBS-NO and observed SST and rainfall; dots in Figures 2e and 2f show that correlation is significantly different from zero at the 95% confidence level according to a Student's *t* test.

The links between REOF-3 of the ensemble mean of OBS-NO and observed SST and rainfall are investigated (Figures 2e and 2f). Here we use the time series from the ensemble mean instead of ERA-Interim because the signal-to-noise ratio is increased in the ensemble mean. It is apparent that this mode is linked to SST variations in the northern Indian Ocean and the western tropical North Pacific. The correlation with precipitation (Figure 2f) displays a tripole pattern with the centers of action located at the Maritime continent, the western tropical North Pacific and East Asia. We also checked the links with SST and precipitation using the RPC corresponding to REOF-2 of ERA-Interim, and results are broadly similar (Figure S5). The distribution of rainfall anomalies (Figure 2f) closely resembles the diabatic heating anomalies driving the interannual fluctuation of the East Asian summer (JJA; austral winter) monsoon associated with the P-J pattern [see *Sun et al.*, 2010, Figure 5a]. *Lin* [2009] examined the global atmospheric circulation response to a diabatic heating anomaly near the Philippines (Figure 2f) using the simple general circulation model described in his paper. The results show that the heating anomaly does indeed generate a SH wave train similar to that in Figures 2a and 2b and also the P-J pattern in East Asia (refer to Figure 8 in *Lin* [2009]). It follows that the common anomalous rainfall pattern associated with the P-J pattern and REOF-2 of ERA-Interim (REOF-3 of the ensemble mean of OBS-NO) is likely the reason causing a significant correlation between them.

In ERA-Interim, REOF-3 explains 11.7% of the variance and depicts a wave train from the South Pacific to the Amundsen Sea, reminiscent of the Pacific-South American (PSA) teleconnection [*Karoly*, 1989]. Compared with EOF-3 (Figure S1), the varimax rotation reduces and enhances the loading of action in the Indian Ocean and Pacific sector, respectively, so that REOF-3 manifests as a localized pattern in the Pacific sector (Figure 3a).
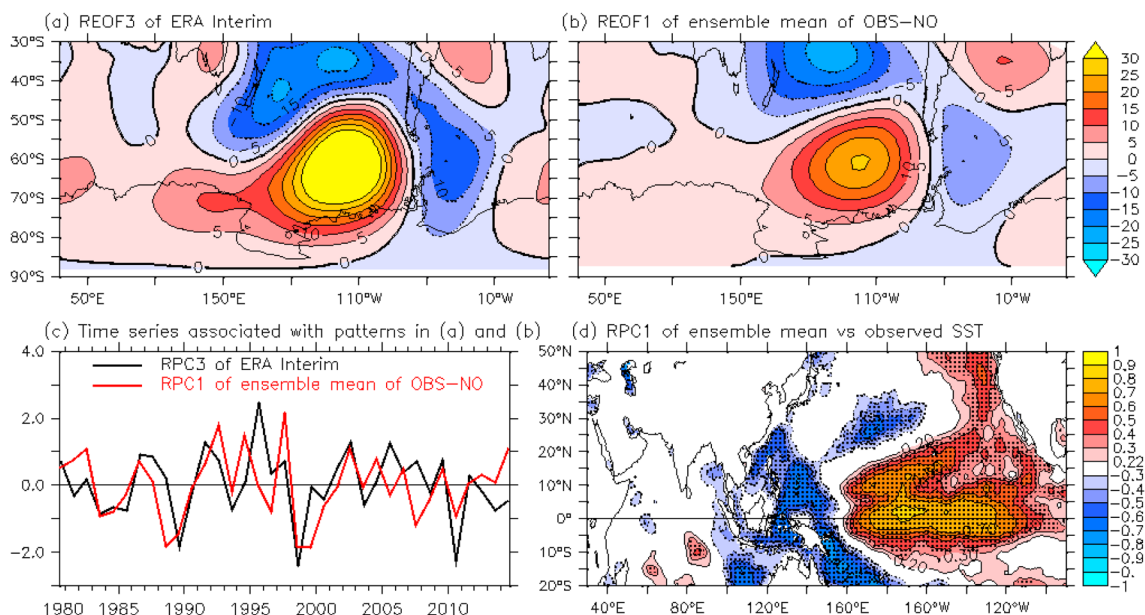
**Figure 3.** Spatial patterns of (a) REOF-3 of ERA-Interim (explaining 11.7% of the variance), (b) REOF-1 of the ensemble mean of OBS-NO (explaining 30.9% of the variance), and their principal components are shown in Figure 3c. (c) The RPCs are normalized by their own standard deviation which is now carried by the corresponding spatial pattern shown in Figures 3a and 3b. (d) The correlation between RPC-1 of the ensemble mean of OBS-NO and observed SST; dots in Figure 3d show that correlation is significantly different from zero at the 95% confidence level according to a Student's *t* test.

*Ding et al.* [2012] indicated that SST variability in the central tropical Pacific impacts the SH climate via the PSA pattern. The ensemble mean of OBS-NO captures the PSA pattern as its REOF-1 (Figure 3b), explaining 30.9% of the variance, suggesting that the SST-forced external component strongly projects onto the PSA pattern. The RPCs associated with REOF-3 of ERA-Interim and REOF-1 of the ensemble mean are shown in Figure 3c. The correlation between the two time series is around 0.47 (significantly different from zero at the 95% confidence level). It follows that the ensemble mean captures about 25% of the variance associated with the observed PSA pattern with the suggestion from Figure 3c of a clearer link at decadal than at interannual time scales. The time evolution of the PSA in the ensemble mean is significantly associated with SST (Figure 3d) and rainfall (not shown) variations in the tropical central Pacific, consistent with *Ding et al.* [2012]. The correlations are also calculated using the RPC of REOF-3 of ERA-Interim, and the relationship with SST and rainfall in the central tropical Pacific is still significant (Figure S5).

## 4. Summary and Discussion

In this study, we examined the interannual variability of the extratropical Southern Hemisphere atmospheric circulation during austral winter, which has received little attention. Both observations and an ensemble of nine integrations by an atmospheric model forced with global observed sea surface temperature (SST) are employed. The ensemble of experiments is referred to as OBS-NO. In the experiments, the ensemble mean is taken to be the SST-forced component, while deviations from the ensemble mean are taken to be internal components. One caveat is that the ensemble mean of nine ensemble members may not be enough to remove all internal variations; we should bear this in mind when looking at the ensemble mean.

Our analyses show that in ERA-Interim, austral winter atmospheric circulation interannual variability is depicted by the three major modes identified through rotated EOF (REOF) analysis. The Southern Annular Mode (SAM) is captured by REOF-1 as the dominant mode, and its existence is attributed mainly to internal dynamics [e.g., *Thompson and Wallace*, 2000], which is further corroborated by noting that the SAM is the dominant mode (REOF-1) of the internal component of the model experiment and that the ensemble mean fails to capture a significant part of the variations associated with the observed SAM. In ERA-Interim, REOF-2 is marked by a wave train emanating from Australia to the South Pacific, and REOF-3 is regarded as the Pacific-South American pattern. Furthermore, REOF-2 displays an interhemispherical link with the western North Pacific summer (JJA; boreal season) monsoon and even the Pacific-Japan pattern which is the leading mode of the East Asian summer (JJA; boreal season) monsoon [*Sun et al.*, 2010]. We note that externally forced variability

strongly projects onto both REOF-2 and REOF-3 so that the ensemble mean of OBS-NO captures a considerable part of the interannual variability associated with REOF-2 (50%) and REOF-3 (25%) in ERA-Interim. Additionally, we have also projected the ensemble mean of OBS-NO onto the spatial patterns of the first three REOFs calculated from ERA-Interim. The correlation between the principal components of ERA-Interim and the derived time series by the projection onto the corresponding REOF spatial patterns shows little change to that reported above (Figure S6). Finally, we note that our results have importance for predictability studies of the extratropical SH climate.

## References

Baldwin, M. P. (2001), Annular modes in global daily surface pressure, *Geophys. Res. Lett.*, *28*(21), 4115–4118, doi:10.1029/2001GL013564.

Dee, D. et al. (2011), The ERA-Interim reanalysis: Configuration and performance of the data assimilation system, *Q. J. R. Meteorol. Soc.*, *137*(656), 553–597, doi:10.1002/qj.828.

Ding, H., R. J. Greatbatch, and G. Gollan (2015), Tropical impact on the interannual variability and long-term trend of the Southern Annular Mode during austral summer from 1960/1961 to 2001/2002, *Clim. Dyn.*, *44*(7–8), 2215–2228, doi:10.1007/s00382-014-2299-x.

Ding, Q., and E. J. Steig (2013), Temperature change on the Antarctic Peninsula linked to the tropical Pacific*., *J. Clim.*, *26*(19), 7570–7585, doi:10.1175/JCLI-D-12-00729.1.

Ding, Q., E. J. Steig, D. S. Battisti, and J. M. Wallace (2012), Influence of the tropics on the Southern Annular Mode, *J. Clim.*, *25*(18), 6330–6348, doi:10.1175/JCLI-D-11-00523.1.

Fogt, R. L., and D. H. Bromwich (2006), Decadal variability of the ENSO teleconnection to the high-latitude South Pacific governed by coupling with the Southern Annular Mode, *J. Clim.*, *19*(6), 979–997, doi:10.1175/JCLI3671.1.

Grassi, B., G. Redaelli, and G. Visconti (2005), Simulation of polar Antarctic trends: Influence of tropical SST, *Geophys. Res. Lett.*, *32*(23), L23806, doi:10.1029/2005GL023804.

Kalnay, E., et al. (1996), The NCEP/NCAR 40-year reanalysis project, *Bull. Am. Meteorol. Soc.*, *77*(3), 437–471, doi:10.1175/1520-0477(1996)077<0437:TNYRP>2.0.CO;2.

Karoly, D. J. (1989), Southern Hemisphere circulation features associated with El Niño–Southern Oscillation events, *J. Clim.*, *2*(11), 1239–1252, doi:10.1175/1520-0442(1989)002<1239:SHCFAW>2.0.CO;2.

L'Heureux, M. L., and D. W. Thompson (2006), Observed relationships between the El Niño–Southern Oscillation and the extratropical zonal-mean circulation, *J. Clim.*, *19*(2), 276–287, doi:10.1175/JCLI3617.1.

Li, C., R. Lu, and B. Dong (2012), Predictability of the western North Pacific summer climate demonstrated by the coupled models of ENSEMBLES, *Clim. Dyn.*, *39*(1–2), 329–346, doi:10.1007/s00382-011-1274-z.

Li, C., R. Lu, and B. Dong (2014), Predictability of the western North Pacific summer climate associated with different ENSO phases by ENSEMBLES multi-model seasonal forecasts, *Clim. Dyn.*, *43*(11–12), 1829–1845, doi:10.1007/s00382-013-2010-7.

Li, C., R. Lu, and B. Dong (2015), Interdecadal changes on the seasonal prediction of the western North Pacific summer climate around the late 1970s and early 1990s, *Clim. Dyn.*, 1–14, doi:10.1007/s00382-015-2711-1.

Lin, H. (2009), Global extratropical response to diabatic heating variability of the Asian summer monsoon, *J. Atmos. Sci.*, *66*(9), 2697–2713, doi:10.1175/2009JAS3008.1.

Lu, R., Y. Li, and B. Dong (2006), External and internal summer atmospheric variability in the western North Pacific and East Asia, *J. Meteorol. Soc. Jpn.*, *84*(3), 447–462, doi:10.2151/jmsj.84.447.

Nitta, T. (1987), Convective activities in the tropical western Pacific and their impact on the Northern Hemisphere summer circulation, *J. Meteorol. Soc. Jpn.*, *65*(3), 373–390.

North, G. R., T. L. Bell, R. F. Cahalan, and F. J. Moeng (1982), Sampling errors in the estimation of empirical orthogonal functions, *Mon. Weather Rev.*, *110*(7), 699–706, doi:10.1175/1520-0493(1982)110<0699:SEITEO>2.0.CO;2.

Rowell, D. P., C. K. Folland, K. Maskell, and M. N. Ward (1995), Variability of summer rainfall over tropical North Africa (1906–92): Observations and modelling, *Q. J. R. Meteorol. Soc.*, *121*(523), 669–704, doi:10.1002/qj.49712152311.

Sun, X., R. Greatbatch, W. Park, and M. Latif (2010), Two major modes of variability of the East Asian summer monsoon, *Q. J. R. Meteorol. Soc.*, *136*(649), 829–841, doi:10.1002/qj.635.

Thompson, D. W., and J. M. Wallace (2000), Annular modes in the extratropical circulation. Part I: Month-to-month variability*, *J. Clim.*, *13*(5), 1000–1016, doi:10.1175/1520-0442(2000)013<000:AMITEC>2.0.CO;2.

von Storch, H., and F. W. Zwiers (2002), *Statistical Analysis in Climate Research*, vol. 1, 494 pp., Cambridge Univ. Press, Cambridge, U. K.

Wang, B., and Z. Fan (1999), Choice of South Asian summer monsoon indices, *Bull. Am. Meteorol. Soc.*, *80*(4), 629–638, doi:10.1175/1520-0477(1999)080<0629:COSASM>2.0.CO;2.

Zhou, T., and R. Yu (2004), Sea-surface temperature induced variability of the Southern Annular Mode in an atmospheric general circulation model, *Geophys. Res. Lett.*, *31*(24), L24,206, doi:10.1029/2004GL021473.